A photon conversion finder at BESIII*

XU Zhi-Rui(许志蕊)[1;1)] HE Kang-Lin(何康林)[2]

[1] State Key Laboratory of Particle Detection & Electronics, University of Science and Technology of China, Hefei 230026, China
[2] Institute of High Energy Physics, Chinese Academy of Sciences, Beijing 100049, China

Abstract: A photon conversion finder (PCF) based on track information from the main drift chamber (MDC) of the Beijing Spectrometer (BESIII) at the Beijing Electron Positron Collider (BEPC II) is developed. The validation of the PCF is done by reconstructing π^0 and measuring the branching fraction of $J/\psi \to \gamma\eta'$. Using the developed PCF tool, we mapped the materials from the interaction point through the BEPCII beam pipe up to the inner wall of the MDC.

Key words: photon conversion, material mapping, BESIII detector

PACS: 07.05.Kf **DOI:** 10.1088/1674-1137/36/8/010

1 Introduction

Photons with an energy greater than twice the mass of the electron ($E_\gamma > 1.02$ MeV) have a finite probability to convert into an electron positron pair through the process $\gamma A \to e^+e^-A$ when they are in the presence of a Coulomb field of the nucleus of the material with atomic number A. For photons with energy above 10 MeV, pair conversion is the dominant interaction process [1]. The probability of conversion is directly related to the intensity of the electromagnetic field encountered by the photons. Thus photons converted in the material of the detector with a rate proportional to the radiation length reveals the macroscopic properties of the material traversed.

Reconstruction of the converted photon is often used for detector-related studies such as mapping the material of the detector with the vertices reconstructed from e^+e^- pair of the photon conversion; physics analysis for the process with photons such as the radiative decay process $X^* \to \gamma X$.

This work is aiming at building a proper photon conversion finder (PCF), using the e^+e^- pairs detected with MDC, for the BESIII detector, which may play an important role in validating the material input in the Monte Carlo simulation of the detector.

In Section 2 we briefly describe the BESIII detector, particularly the MDC and the beam pipe of the accelerator inside the MDC. The algorithm for the photon conversion finder and the efficiency for the detection of the converted photon are described in Section 3. In Section 4 we validate the PCF by reconstructing π^0, measuring the branching fraction of $J/\psi \to \gamma\eta'$ with the radiative photon detected based on the photon conversion. The BESIII material mapping from the beam pipe up to the inner wall of the MDC, using the PCF, is depicted in Section 5.

2 The BESIII detector

The BESIII detector with a geometrical acceptance of 93% of 4π has four main components: (1) A small-cell, helium-based drift chamber with 43 layers providing an average single-hit resolution of 135 μm, charged-particle momentum resolution in a 1 T magnetic field of 0.5% at 1 GeV/c, and the dE/dx resolution that is better than 6%. (2) An electromagnetic calorimeter (EMC) consisting of 6240 CsI(Tl) crystals in a cylindrical structure (barrel) and two end caps. The energy resolution at 1.0 GeV/c is 2.5% (5%) in the barrel (endcaps), and the position resolution is 6 mm (9 mm) in the barrel (endcaps). (3) A time-of-

Received 1 November 2011, Revised 12 December 2011
* Supported by National Natural Science Foundation of China (10875113, 10875138, 11079030, 11179007)
1) E-mail: xuzr@ihep.ac.cn

flight (TOF) system composed of 5 cm thick plastic scintillators, with 176 detectors of 2.4 m long in two layers in the barrel and 96 fan-shaped detectors in the endcaps. The barrel (endcap) time resolution of 80 ps (110 ps) provides 2σ K/π separation for momenta up to $\sim$1.0 GeV/c. (4) A muon counter (MUC) consists of 1000 m^2 of resistive plate chambers in nine barrel and eight endcap layers and provides 2 cm position resolution. Since the material mapping will be done up to the inner wall of the MDC, we present the detailed information for the structure and the corresponding materials inside it in Section 2.1 and Section 2.2. More detailed information about the detector can be found in Ref. [2].

2.1 The beam pipe

The structure of the beam pipe [3] has a total length of 1000 mm and an inner diameter of Φ63 mm. The beryllium beam pipe is composed of a 0.8 mm thick inner beryllium pipe which is coated with 14.6 μm gold, a 0.6 mm thick outer beryllium pipe, and two copper extension pipes at both ends. A special paraffin oil or synthetic machine oil SMO-1 (sparking machining oil No.1) chosen as the coolant for the beryllium beam pipe fills the narrow cooling gap between the inner and outer beryllium beam pipes. The total thickness that particles produced at the IP must penetrate corresponds to 1.04% (Be: 0.4%, gold: 0.44%, SMO: 0.2%) of a radiation length at normal incidence.

2.2 The MDC

As the innermost sub-detector of BESIII detector, the MDC [3] consists of two parts, an inner chamber and an outer chamber with the polar angle coverage of the innermost and outermost wires being $|\cos\theta| \leqslant 0.93$ and $|\cos\theta| \leqslant 0.83$, respectively. It adopts the multilayer small cell drift chamber design. The outer radius of the MDC is chosen to be 810 mm and the inner radius 59 mm. The stepped structure end plate of the inner chamber is made of aluminum (Al-7075) with a thickness of 25 mm. The inner skin of the chamber is made of carbon fiber, 1 mm thick ($0.45\%X_0$). A helium based gas mixture He/C_3H_8 60:40 is chosen to be the drift chamber gas.

Figure 1 shows the locations of photon conversions in the BESIII detector as found in the true Monte Carlo (only photons interacting with detector materials are handled by Geant4 but without tracking electrons) from a sample of 0.5 GeV single photon events. Electron-positron pairs from the converted photons which can be detected by the MDC are mainly from the beam pipe and the inner MDC wall. This can be clearly seen in the plot.

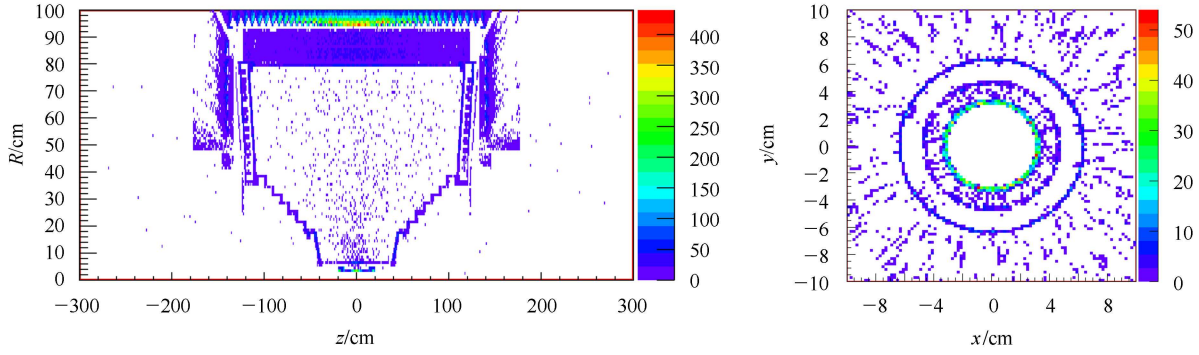

Fig. 1. Mapping of the BESIII detector using photon conversion (Monte Carlo true information).

3 The photon conversion finder

Charged tracks reconstructed from MDC are required to be in the polar angle region $|\cos\theta| < 0.93$. In order to reject beam related backgrounds, tracks are also required to be originated within ±30 cm of the interaction point (IP) in the beam direction. Candidate events must have no less than two charged tracks.

In order to suppress the hadronic charged tracks background, electron identification based on the combined information of MDC (dE/dx), TOF, EMC and MUC from the sub-detectors is performed to calculate χ^2 values and the corresponding confidence levels prob(x) with an electron/muon/pion/kaon/proton assumption, where x (x=e/μ/π/K/p) isthe particle

type [4]. To identify an electron/positron, the probability prob(e) is required to be greater than 0.1% and prob(x) (where x means μ, π, K and p).

Tracks are looped over and combined into pairs. Any two oppositely charged tracks which survive after electron identification will be considered as electron/positron candidates from converted photons.

If we extrapolate and project a pair's trajectories onto x-y plane, they are circles tangent with each other at the point where the photon converts. Based on this, we define Δ_{xy} [5, 6] to be the minimum distance between the electron and positron tracks in x-y plane and Δ_z [5, 6] in z direction. Δ_{xy} and Δ_z are expected to be around zero.

As photons have zero mass, the signature of a conversion is two tracks with a zero opening angle that originates in the material of the detector, i.e., electron-positron tracks are parallel if they are not bending in the magnetic field. $\xi_{\rm ep}$ [7] is defined as the opening angle which is the angle between the momentum vector of the electron and that of the positron.

$$\xi_{\rm ep} = \arccos\left(\frac{\vec{p_{\rm e^+}}\cdot\vec{p_{\rm e^-}}}{|\vec{p_{\rm e^+}}|\cdot|\vec{p_{\rm e^-}}|}\right). \tag{1}$$

But actually, because of the improper reconstruction of the electron's transverse momentum, the pair acquires an artificial azimuthal opening angle. This angle leads to a "mass" m_γ for the reconstructed photon.

If we define the azimuthal opening angle Δ_{ϕ_0} of the $\rm e^+e^-$-pair as the azimuthal angle of the electron $\phi_0(\rm e^-)$ minus the azimuthal angle of the positron $\phi_0(\rm e^+)$:

$$\Delta_{\phi_0} = \phi_0(\rm e^-) - \phi_0(\rm e^+), \tag{2}$$

and the polar opening angle Δ_{θ_0} as:

$$\Delta_{\theta_0} = \theta_0(\rm e^-) - \theta_0(\rm e^+), \tag{3}$$

where $\theta_0(\rm e^-)$ is the polar angle of electron and $\theta_0(\rm e^+)$ that of positron, then we can easily get the angle $\psi_{\rm pair}$ [7] between the plane defined by the momentum vectors of the electron and the positron in which the pair splits up and the plane perpendicular to the magnetic field which is the x-y plane in the coordinate system:

$$\psi_{\rm pair} = \arcsin\left(\frac{\Delta_{\theta_0}}{\xi_{\rm ep}}\right), \tag{4}$$

$\psi_{\rm pair}$ is a measure for the contribution of the opening in polar direction Δ_{θ_0} to the opening angle $\xi_{\rm ep}$. Photon conversions will have a sharp distribution around zero radians in $\psi_{\rm pair}$ and other events a rather flat distribution.

Because most of the photons come from IP, in order to further suppress the background from decays such as $\pi^0 \to \rm e^+e^-\gamma$, an extra parameter $\theta_{\rm eg}$ is defined which is the angle between the vector of the reconstructed photon and the direction from IP to the reconstructed conversion point.

Without considering correlations between cuts, we studied the parameters using Monte Carlo events and defined a set of cuts. The electron pair candidates which satisfy the criteria listed below are considered to originate from a conversion photon.

- -2 cm$< \Delta_{xy} <1$ cm
- $\Delta_z < 2$ cm
- $m_\gamma < 0.05$ GeV/c^2
- $\xi_{\rm ep} < 0.5$
- $|\psi_{\rm pair}| < 0.5$
- $\cos\theta_{\rm eg} > 0.8$

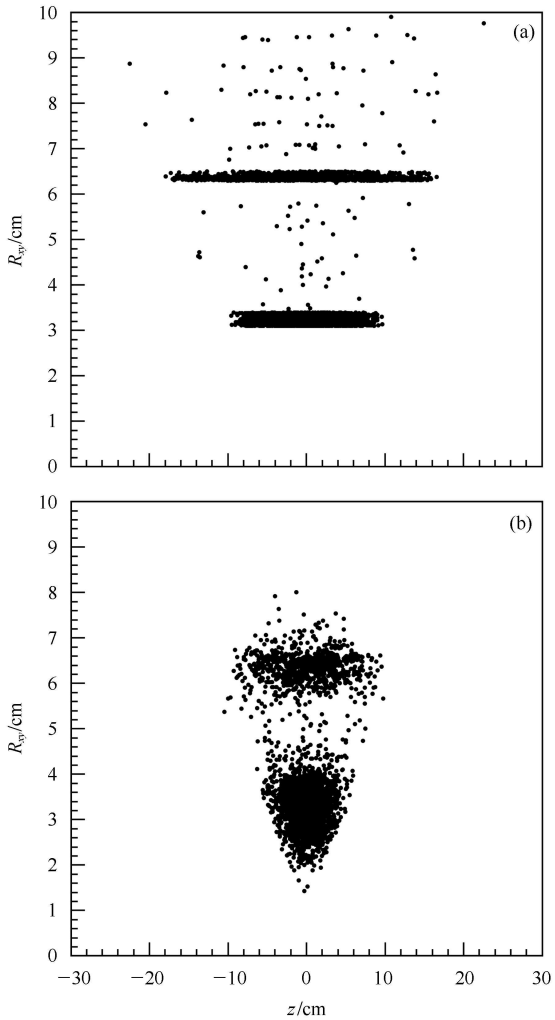

Fig. 2. The reconstructed photons in R-z plane. (a) Monte Carlo truth; (b) Monte Carlo reconstructed.

Two dimensional plots for reconstructed photons in the R-z plane and x-y plane are shown in Fig. 2 and Fig. 3, which means we have successfully built the finder.

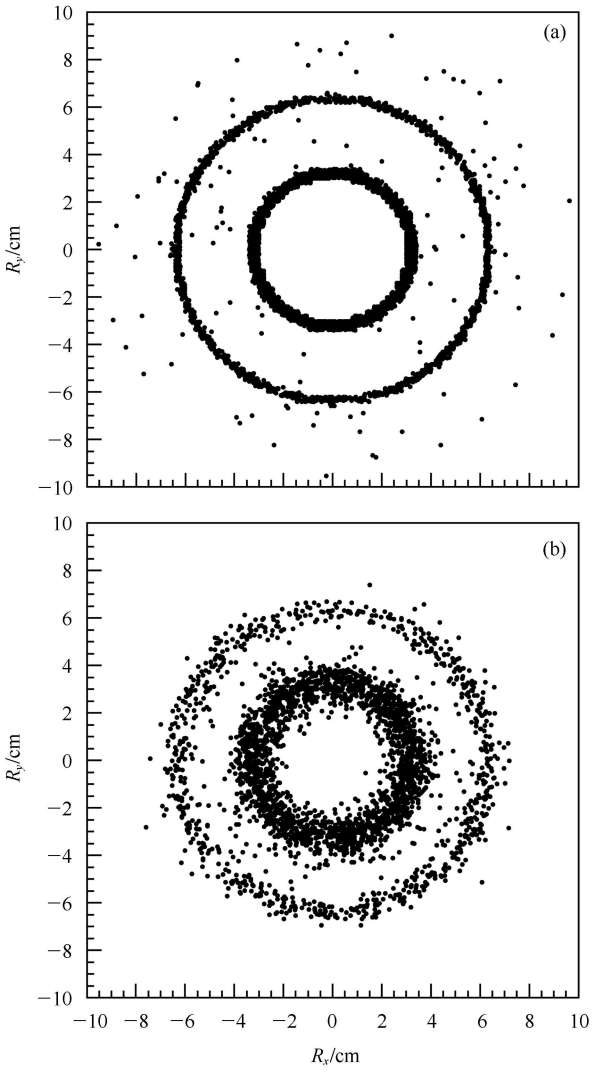

Fig. 3. The reconstructed photons in x-y plane. (a) Monte Carlo truth; (b) Monte Carlo reconstructed.

Single energy photon with a uniform angular distribution in the full geometry space at each energy point was used for the PCF efficiency study. As shown in Fig. 1, most of the conversions occur out of the geometrical acceptance of the MDC. Considering the general track cuts used, we demand $|\cos\theta|<0.93$ and $|z|<30$ cm for electron and positron tracks and $R_{xy}<10$ cm for the conversion photons in Monte Carlo truth. The conversion detection efficiency ϵ is defined as:

$$\epsilon=\frac{N^{\rm gconv}}{N^{\rm MC}}, \qquad (5)$$

where $N^{\rm gconv}$ is the number of reconstructed converted photons; $N^{\rm MC}$ is the number of generated Monte Carlo events in the detector geometry acceptance, i.e., those events that passed the general track cuts. It includes the efficiencies like tracking and pair selection. The result is shown in Fig. 4.

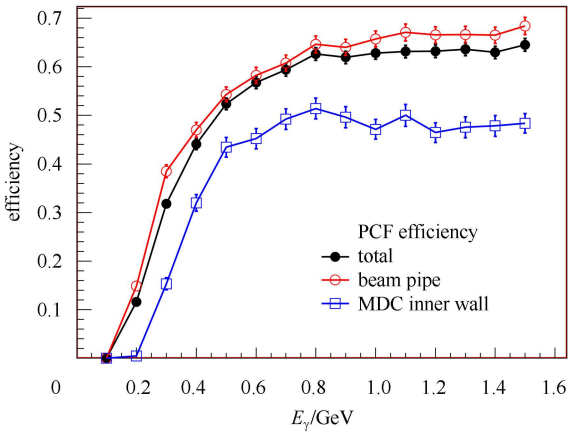

Fig. 4. The converted photon detection efficiency.

4 Validation of PCF

4.1 Reconstruction of π^0

π^0 is largely produced in BESIII experiment. We have enough data to do a most accurate measurement of π^0 with both photons producing conversion pairs. After reconstruction of two converted photons, an extra cut f_{π^0}, which is defined as the absolute value of $\frac{E_{\gamma1}-E_{\gamma2}}{p_{\pi^0}}$, is required to be less than 0.95 to remove background events in which a π^0 is falsely reconstructed from a high energy photon and second spurious shower. Fig. 5 shows the final invariant mass distribution of $\gamma\gamma$ and clear π^0 and η signals are seen.

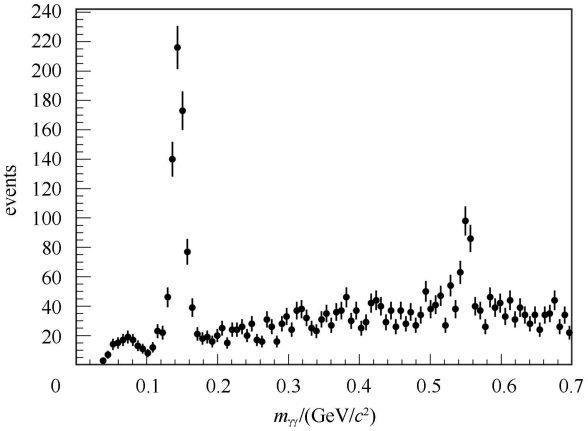

Fig. 5. Invariant mass spectrum of $\gamma\gamma$.

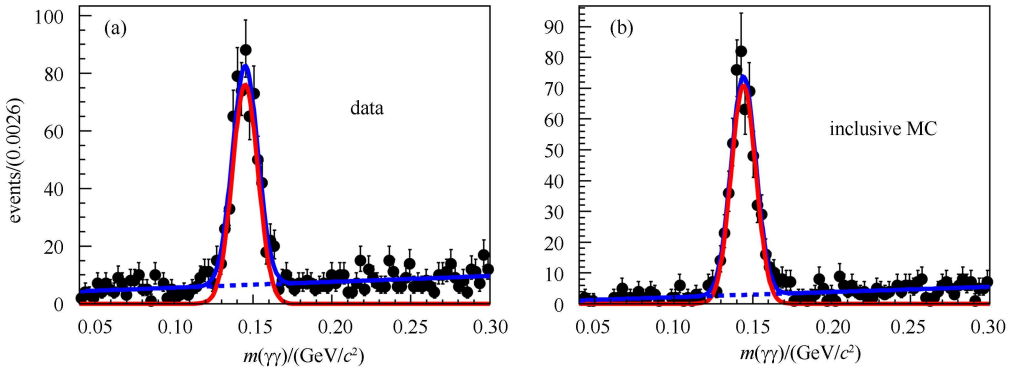

Fig. 6. The fitting of π^0 signal.

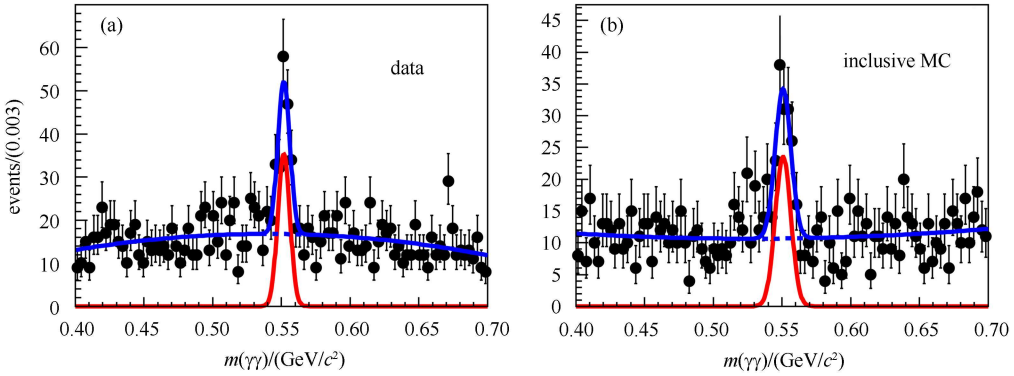

Fig. 7. The fitting of η signal.

Single Gaussian plus a polynomial function where Gaussian function describes signals and polynomial function describes the background is used to fit the $\gamma\gamma$ mass spectra (Fig. 6 and Fig. 7) and the results are listed in Table 1 and Table 2. The reconstructed π^0 mass is about 10 MeV higher than the PDG [8] value and η mass is about 4 MeV higher.

Table 1. The fitting results of π^0 signal.

	#signal	mass/MeV	sigma/MeV
DATA	591 ± 27	145.09 ± 0.40	8.07 ± 0.36
inclusive MC	532 ± 25	144.21 ± 0.39	7.79 ± 0.34

Table 2. The fitting results of η signal.

	#signal	mass/MeV	sigma/MeV
DATA	128 ± 17	551.82 ± 0.65	4.37 ± 0.64
inclusive MC	112 ± 17	550.83 ± 0.99	5.70 ± 1.01

Electron-positron pairs originating at different positions of π^0 are studied (Table 3). The result shows the effect of different positions of conversion which occurred for photons.

4.2 The branching fraction of $J/\psi\to\gamma\eta'$

The photon conversion finder is used to study the η' signal in J/ψ radiative decays. If the photon converts, it will have two extra charged tracks. We reconstruct the photon based on these two tracks using PCF. Fig. 8 is the photon recoil mass spectra. Clear η' signal is shown in the recoil mass spectra of reconstructed photons.

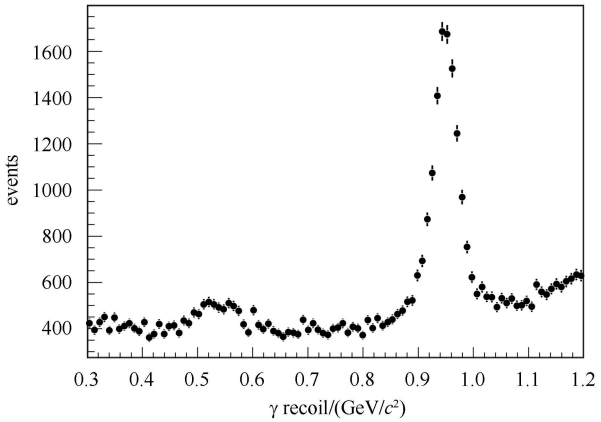

Fig. 8. Recoil mass spectra of the reconstructed converted photon.

We apply a simple fit to η' mass spectra (Fig. 9) using function

$$BW(m;m_0,\Gamma_0)\otimes G(m;\sigma)+B, \quad (6)$$

where $BW(m;m_0,\Gamma_0)$ is the natural line shape of the resonance of η'. $G(m;\sigma)$ describes the instrumental mass resolution function. B describes the flat background. The natural widths of the η' states are fixed according to PDG while their masses and resolutions are free parameters to be determined. The fitting results are shown in Table 4. The mass of the reconstructed η' is about 8 MeV lower than the PDG value (957.66±0.24 MeV/c^2). η' performs in the opposite way to π^0 and η because we study the recoil mass of the converted photons here.

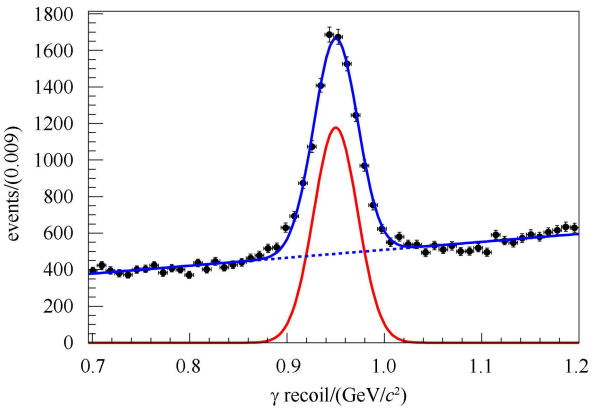

Fig. 9. The fitting of the η' signal.

We generated 0.5 million $J/\psi\to\gamma\eta'$ Monte Carlo sample to study the detection efficiency of η' using converted photons. The efficiency is $(0.48\pm0.01^{\rm stat.})\%$ and the branching fraction is measured to be $(5.31\pm0.21^{\rm stat.})\times10^{-3}$ which is consistent with the PDG value $(5.28\pm0.15)\times10^{-3}$.

4.3 The dE/dx correction

No vertex tracker is a shortage for the BESIII detector in the detection of photon conversions since conversion occurs wherever photons encountered material. For the BESIII MDC tracking, it chose the innermost fired wire as the pivot in track fitting and then extrapolated the track back to IP. Issues such as material effects, non-uniform magnetic field wire sagita, are done using the Kalman Filter method [9]. Our PCF uses the track's helix parameters read out after the Kalman Filter. So there might be two reasons to cause the invariant mass shift for π^0, η and η': one is that the energy loss is overestimated for electron tracks and the other is that the transverse momentum of the tracks is improperly reconstructed.

By studying the electron-positron pairs originating at the beam pipe and MDC inner wall separately which are shown in Table 3 and Table 4, we can conclude that dE/dx is really improperly corrected for the electrons from converted photons. Considering

Table 3. Electron-positron pairs of photons from π^0 decays originating at different position.

position	#signal	mass/MeV	sigma/MeV
BP+BP[1]	264±18	141.18±0.40	5.32±0.40
BP+MI[2]	237±17	147.52±0.51	6.44±0.51
MI+MI[3]	47±8	154.59±0.89	5.25±0.80

1 BP+BP: both photons converted at beam pipe;
2 BP+MI: one photon converted at beam pipe and the other at MDC inner cylinder;
3 MI+MI: both photons converted at MDC inner cylinder.

Table 4. The fitting results of η' signal.

position	#event	mass/MeV	width/MeV	sigma/MeV
total	7426±130	950.00±0.11	0.205	22.52±0.43
beam pipe	3379±78	952.80±0.53	0.205	21.39±0.52
MDC inner	2344±64	946.01±0.64	0.205	21.68±0.63

Table 5. Invariant mass comparison before and after dE/dx correction.

particle type	dE/dx correction		PDG/(MeV/c^2)
	old/(MeV/c^2)	new/(MeV/c^2)	
$\eta'(958)$	950.06±0.41	954.37±0.41	957.66±0.24
π^0	145.09±0.40	143.68±0.33	134.9766±0.0006
η	551.82±0.65	548.70±0.57	547.853±0.024

dE/dx corrected too much for electron tracks, a new dE/dx correction approach is needed. We got the track's helix information at the first layer of the MDC and extrapolated it to IP by considering the ionization and multi-scattering for energy loss from the MDC first layer to the conversion point. In Table 5, after new dE/dx correction, the results are better.

5 The material mapping

The Monte Carlo simulation of BESIII detector is fulfilled by a GEANT4-based software BOOST [10]. It includes the geometric and material description of detectors, detector response, and digitization models, as well as the tracking of the detector running conditions and performance. The production of J/ψ and ψ′ resonances are simulated by the Monte Carlo event generator KKMC [11], while the decays are generated by EVTGEN [12] for known modes with branching fractions being set to the PDG world average values and by LUNDCHARM [13] for the remaining unknown decays. From the previous section, we have enough statistics to do a detector material scan using photons coming from $J/\psi \to \gamma\eta'$ channel. R_{xy} distributions of real data and 225 million inclusive Monte Carlo samples generated by the BESIII Monte Carlo group are compared in Fig. 10. From Fig. 10, it can be seen that Monte Carlo and data are consistent with each other very well except a little difference for

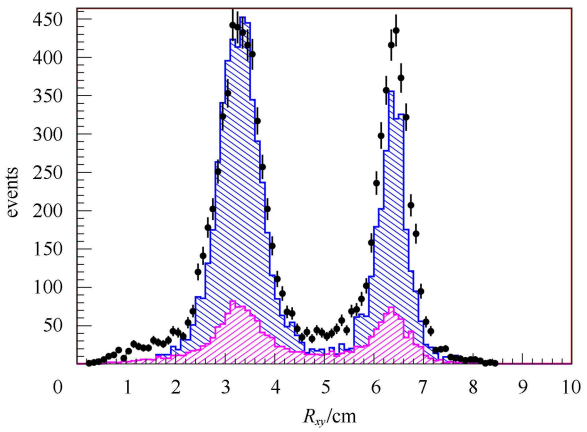

Fig. 10. Distribution of R_{xy} shows that data (black dots) and inclusive Monte Carlo are consistent with each other where $J/\psi \to \gamma\eta'$ signal (blue grid histogram) comes from the inclusive Monte Carlo sample and the contribution from other sources are described by η′ sideband (pink shaded histogram) from data.

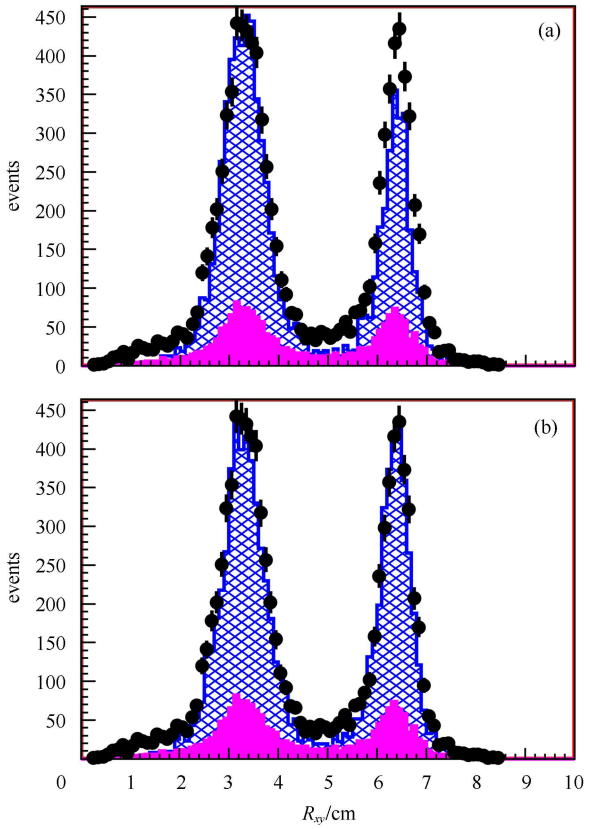

Fig. 11. Two Monte Carlo samples of $J/\psi \to \gamma\eta'$ are generated to study the input of material in simulation: (a) MDC inner cylinder with 1.2 mm carbon fiber (blue grid histogram); (b) MDC inner cylinder with 1.2 mm carbon fiber plus 150 μm aluminum film (blue grid histogram).

the MDC inner cylinder, which means the amount of material implemented in the Monte Carlo simulation might be a little less than the real case. In the Monte Carlo simulation, it has only implemented 1.2 mm carbon fiber for the MDC inner cylinder.

It was found necessary to add a 150 μm aluminum film to the MDC inner wall in Monte Carlo simulation later. Two samples of $J/\psi \to \gamma\eta'$ were generated to study the performance of the Monte Carlo simulation before and after the aluminum film was added: one has only a 1.2 mm carbon fiber for the MDC inner cylinder and the other has a 1.2 mm carbon fiber plus a 150 μm aluminum film. After we added a 150 μm aluminum film to the MDC inner cylinder which is about $0.17\%X_0$ extra in the Monte Carlo simulation, Monte Carlo performs much better (see Fig. 11).

6 Conclusion

We successfully built the photon conversion finder at BESIII. By reconstruction of π^0, η and measuring the branching fraction of $J/\psi \to \gamma\eta'$, the PCF is proved to work well. A new dE/dx correction for the electrons is applied to solve the problem of invariant mass shift for reconstructed resonances, which turns out to be feasible. A material scan of the detector based on this PCF is done. The input of material for the beam pipe and MDC inner wall in the Monte Carlo simulation is consistent with the real detector case after a 150 μm Aluminum film is added.

We wish to thank H. M. Liu, Z. Y. Deng, Y. Yuan for their help on the Monte Carlo simulation and X. Ma and Z. P. Mao on the dE/dx correction. We would also like to thank Y. Zhang, C. D. Fu, T. Ma and many other BESIII members for their useful help. Thanks also go to M. Xu for helping me to start this work. Finally, we wish to express our special thanks to Z. G. Zhao, without whom this work would not been done.

References

1 Perkins D H. Introduction to High Energy Physics. Forth Edition. Cambridge: Cambridge University Press, 2000
2 BESIII Collaboration. The preliminary Design Report of the BESIII Detector. Report No. IHEP-BEPCII-SB-13
3 Ablikim M et al. Nuclear Instruments and Methods in Physics Research A, 2010, **614**: 345–399
4 HUANG Bin. Study of BESIII Offline Calibration and Particle Identification (Ph.D. Thesis). Beijing: Institute of High Energy Physics, CAS, 2009 (in Chinese)
5 Dunwoodie B, Hast C, Lees J-P et al. Study of Material Interactions with Gamma Conversions and Protons. BABAR Analysis Document #106, Version 2
6 Lurie Z. Evaluation of the Photon Conversion Finder for the BABAR Experiment (M.S. Thesis). Vancouver, British Columbia: The University of British Columbia, February 2002
7 Dahms T. Measurement of Photons via Conversion Pairs with the PHENIX Experiment at RHIC (M.S. Thesis). Stony Brook, New York: Stony Brook University, May 2005
8 Nakamura K et al. (Particle Data Group). J. Phys. G, 2010, **37**: 075021
9 WANG D Y et al. Nuclear Electronics and Detection Technology, 2007, **27**: 658–664
10 DENG Z Y et al. HEP & NP, 2006, **30**: 371 (in Chinese)
11 Jadach S, Ward B F L, Was Z. Comput. Phys. Commun., 2000, **130**:260; Phys. Rev. D, 2001, **63**: 113009
12 PING R G et al. Chinese Phys. C (HEP & NP), 2009, **32**: 599
13 CHEN J C, HUANG G S, QI X R et al. Phys. Rev. D, 2000, **62**: 034003